



ISSN: 0975-833X

RESEARCH ARTICLE

HIGH-STEP-UP INTERLEAVED DC-DC CONVERTER WITH COUPLED-INDUCTOR

V. Anto Sahaya Varghese and S. Prathiba

Department of Electrical and Electronics Engineering, Easwari Engineering College, Chennai-89

ARTICLE INFO

Article History:

Received 27<sup>th</sup> April, 2012  
Received in revised form  
15<sup>th</sup> May, 2012  
Accepted 12<sup>th</sup> June, 2012  
Published online 30<sup>th</sup> July, 2012

Key words:

Active-clamp,  
Boost converter,  
Coupled-inductor boost converter,  
Dc-Dc power converter,  
High voltage gain,  
Interleaving.

ABSTRACT

This paper presents a high-efficiency and high-step-up nonisolated interleaved dc-dc converter with a common active-clamp circuit. In the proposed converter, the coupled-inductor boost converters are interleaved. A boost converter is used to clamp the voltage stresses of all the switches in the interleaved converters, caused by the leakage inductances present in the practical coupled inductors, to a low voltage level. The leakage energies of the interleaved converters are collected in a clamp capacitor and recycled to the output by the clamp boost converter. A new topologies and interleaving modulation concepts for multilevel dc-dc boost converter enabling a significantly less loss and a reduced chip size of the power semiconductors are proposed. The proposed converter achieves high efficiency because of the recycling of the leakage energies, reduction of the switch voltage stress, mitigation of the output diode's reverse recovery problem, and interleaving of the converters. A prototype of the proposed converter is developed, and its experimental results are presented for validation.

Copy Right, IJCR, 2012, Academic Journals. All rights reserved.

INTRODUCTION

In many applications, high-efficiency, high-voltage step-up dc-dc converters are required as an interface between the available low voltage sources and the output loads, which are operated at much higher voltages. Examples of such applications are as follows. Different distributed energy storage components such as batteries, fuel cells, and ultracapacitors are used in the power trains of hybrid electric vehicles (HEV), electric vehicles (EV), and fuel cell vehicles (FCV). In the present power train architectures of these vehicles, the voltage levels of the energy storage elements are usually low, whereas the motors of the vehicles are driven at much higher voltages [1]–[4]. Next, the telecom and the computer industry utilize the standard batteries, with low voltage levels, as a back-up power source [5], [6]. In such applications, a front-end converter with dual inputs is used. The dc-dc converter, used in this case, is required to boost the low-input voltage of the batteries to the high voltage of the dc bus. Another example is the automotive headlamps, using the high-intensity discharge lamp ballasts [5], [7].

The dc-dc converter, used in this application, is required to boost the low voltage level of car battery to much higher voltage level during the start-up and normal operations. Finally, few emerging applications, such as photovoltaic cells, also require high-gain dc voltage conversion [8]. It can be noted that in all these applications, the high-step-up dc-dc converters can be nonisolated but they should operate at high efficiency while taking high currents from low-voltage dc sources at their inputs. In a conventional boost converter, the duty ratio increases as the output to input voltage ratio

increases. However, the previously mentioned applications require high-voltage step-up and high-efficiency power conversion. Therefore, the conventional boost converters will require extreme duty ratios to meet the high-voltage step-up requirements [9]–[12]. Under such conditions, it is a major challenge to operate the boost converters at high efficiency [15]. This is because, with the high-output voltage, the boost switch has to block a large voltage and hence the ON-state resistance, RDS-ON, which varies almost proportionally with the square of blocking voltage, will be very high. Furthermore, the low-level input voltages cause large input currents to flow through the switches. The extreme duty-cycle operation drives short-pulsed currents with high amplitude to flow through the output diodes and the capacitors; which cause severe diode reverse recovery problem and increases in the conduction losses. The high RDS-ON of the switches, the increased conduction losses, and the severe reverse-recovery problem will degrade the efficiency and limit the power level of the conventional boost converters [15]. Moreover, the parasitic ringing, present in the practical circuits, induces additional voltage stresses and necessitates the use of switches with higher blocking voltage ratings, which will lead to more losses. The coupled-inductor boost converter can be a good solution to the previously discussed problems of the conventional boost converter is shown in Fig. 1. This is because the turns ratio of the primary inductor (L1) to the secondary inductor (L2) of the coupled inductor can be effectively used to reduce the duty ratio and the voltage stress of the switch [5], [10]. Therefore, for high-voltage step-up applications, the coupled-inductor boost converter can be more efficient than the conventional boost converter. However, for high power applications, handling of very large input currents from the low-input voltage sources remains a

\*Corresponding author: anto\_r31@yahoo.co.in

practical issue. Various converter topologies using magnetically coupled inductors are reported in the literature to reduce to the extreme duty ratio operation for nonisolated high step-up applications [8]–[14]. But they are not suitable for high current and high power applications, and moreover, the circuits are complex to design and model. For high-input current, it can be proposed to interleave the coupled-inductor boost converters to process high power, and to achieve high efficiency and high reliability with reduced size inductors and capacitors [17].

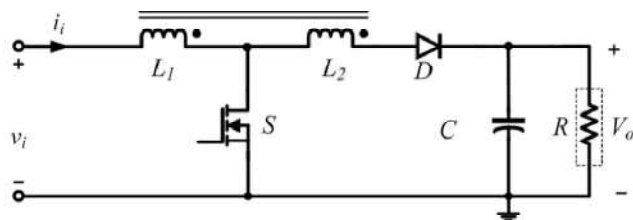


Fig. 1 Coupled-inductor boost converter

Various advantages of interleaving are well reported in the literature [10], [11], and [12]. The schematic diagram of the proposed interleaved coupled-inductor boost converter is shown in Fig. 3. An interleaved boost converter with three winding-based coupled inductors is reported in [11] and [12]. This converter has two interleaved cells, and the inductors of one interleaved cell are coupled with the inductors of the other interleaved cell. Therefore, with this converter the modular structure, which is a key beneficial feature of the interleaved converters, cannot be realized. Furthermore, the maximum number of interleaved cell is only two in this converter.

The interleaved converter, presented in this paper, is modular and can be designed for any number of cell. In a practical coupled inductor, there will be considerable amount of leakage inductance present due to the non-ideal coupling between the primary inductor ( $L_1$ ) and the secondary inductor ( $L_2$ ). The leakage inductance causes high voltage stresses to the switches, large switching losses, parasitic ringing, and severe electromagnetic interference problems, which degrade the converter performances [8] and [18]. Resistor–capacitor–diode (RCD) based snubber circuits can be used to mitigate the problem, but the losses in these circuits are very high [12] and [18]. Active-clamp circuits can be used to address this issue [12]. Moreover, the efficiency improvement in these circuits is limited by the high conduction loss in the active-clamp switches.

A diode and capacitor-based passive-clamp circuit is shown in Fig. 2. In this clamp circuit, the clamp capacitor ( $C_c$ ) is discharged to the output through the secondary side inductor ( $L_2$ ) of the coupled-inductor boost converter. However, the clamp diode ( $D_c$ ), in this circuit, is in series with the coupled inductor. Therefore, it's not only the leakage inductance current, but the total coupled-inductor current, which flows through the clamp diode ( $D_c$ ). This causes large losses in the clamp diode. The clamp diode needs to be rated for the entire large power processed by the coupled-inductor boost converter. This can make the converter operation inefficient for the higher power applications. Furthermore, in this clamp circuit, to take the advantages of the reduced switch voltage stress feature of the coupled-inductor boost converter, the clamp capacitor has to be considerably large, capable of

handling the high amount of charge, and discharge currents of the converter. Also, this will cause additional losses in the clamp capacitor. It can be noted that, if any of the previously discussed clamp circuit is used in the interleaved coupled-inductor boost converter; each of the interleaved phases of the converter will require additional clamp circuit components and control circuits (for active clamp). This will increase the cost, size, and complexity.

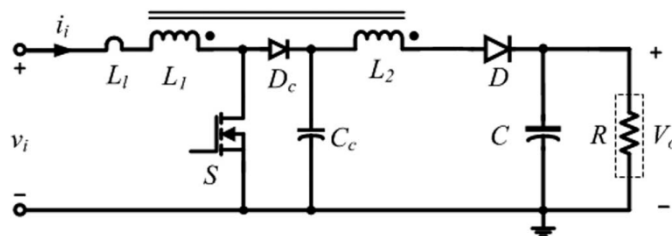
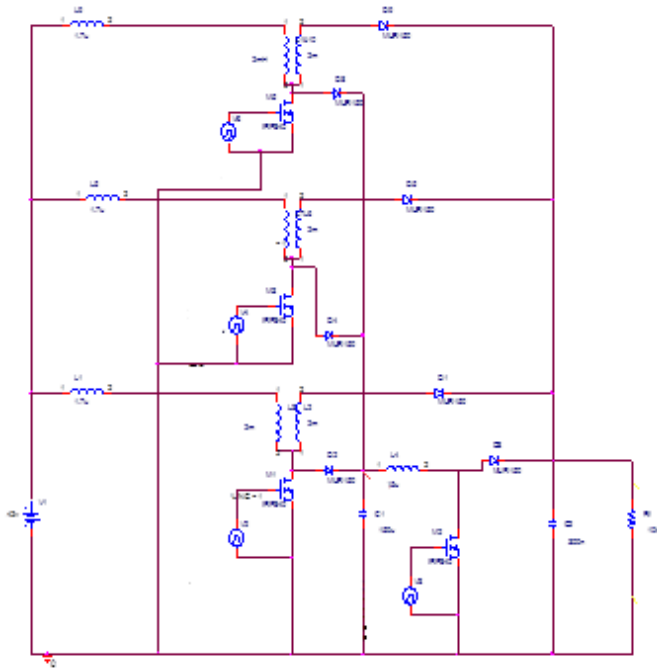


Fig. 2 Coupled-inductor boost converter with clamp circuit

A single active-clamp circuit can be proposed, in which the energy stored in leakage inductances of all the interleaved Coupled-inductor boost converters are gathered in a common clamp capacitor [9]. In each of the interleaved units, a clamp diode is connected from the common node of the coupled inductors to the clamp capacitor for providing the discharge path of the leakage energy. Therefore, only the leakage currents flow through the clamp diodes; this makes the clamping operation efficient. A simple boost converter is used to recycle the leakage energy, gathered in the clamp capacitor, to the output of the interleaved converter. The boost converter is controlled to keep the clamp-capacitor voltage to a low level, and hence, the voltage stress on the switches is low. This allows the use of low-voltage and high-performance devices. It can be noted that, a conventional boost converter can be used for the clamp circuit, because the ratio of the output voltage to the clamp voltage is not very high.

## II. Interleaved coupled-inductor converter

In high current or high power application, interleaving of boost converters are well established. To take benefit of the advantages of interleaving, interleaved coupled-inductor boost converter can be used. In this approach, a single coupled-inductor boost converter cell is treated as a cell and  $n$  such cells are connected in parallel and operated at the same switching frequency. Furthermore, all the cells are operated at the same duty ratio. It can be mentioned that due to interleaving, the effective switching frequency as seen by the input and the output of the interleaved converter circuit is  $n$  times higher than the switching frequency of a phase. Under normal or full-load condition, each of the interleaved cells equally shares the total output load. But under lower output power demand condition, the number of operating cells can be adjusted for maximum efficiency operation of the individual cells. The number of parallel cells  $n$  in an interleaved converter mainly depends on the maximum power demand of the load and the maximum power rating of the interleaved cell. In the practical coupled inductors, due to the nonideal coupling between the primary and the secondary windings, there will be leakage inductances. This leakage inductance will cause high-voltage spikes when the switch is turned off.



**Fig. 3 Proposed interleaved coupled-inductor boost converter with single boost converter clamp**

This results in a high-voltage stress across the switches and in ringing losses. It can be proposed to clamp the switch voltage to the output voltage, using a parallel diode. In this clamp circuit, the energy stored in the leakage inductance is discharged directly to the output by the parallel diode, and the switch voltage is clamped to the output voltage. It can be seen that this converter avoids the disadvantage of series conduction loss of the total power, but the switch voltage stress becomes equal to the output voltage. So this configuration does not take full advantages of the coupled-inductor boost topology, and hence, it is not suitable for high-step-up application where the output voltage level is high. The output voltage is given by,

$$V_o = V_s + L \Delta I / t_2 = V_s (1 + t_1 / t_2)$$

Peak to peak voltage is given by,

$$\Delta V_c = 1/C \int_0^{t_1} I_o dt = I_o t_1 / C$$

$$\Delta V_c = I_o (V_o - V_s) / V_o f C = I_o K / f C$$

To lower the voltage stress on the switches close to the level of the voltage stress present in an ideal coupled-inductor boost converter, a common active-clamp circuit based on a boost converter can be proposed, as shown in Fig. 4. In the proposed active-clamp circuit, in each cell, a clamp-diode (Dc1, Dc2, . . . Dcn) is connected to the common node of the primary inductor, the secondary inductor, and the switch of an interleaved coupled-inductor boost converter. The cathode terminals of all the clamp diodes are connected to a clamp capacitor Cc. The energies stored in the leakage inductors of the interleaved phases are discharged through the clamp diodes and gathered in the clamp capacitor Cc. Furthermore, the boost converter is used to transfer the stored energy in the clamp capacitor to the output of the interleaved converters, while maintaining the voltage level of the clamp capacitor to a lower level is shown in Fig. 3. The voltage stress on the switches (S1, S2, . . . Sn) is decided by this clamp-capacitor

voltage. It can be suggested that any other converter topology, which can perform similar boost operation while maintaining the voltage level of the clamp capacitor can be also used for the active-clamp operation.

### III. Clamp boost converter

From the previous analysis, it can be seen that the energy stored in all the leakage inductances of the interleaved coupled-inductor boost converters are discharged to the capacitor (Cc). To clamp the switch voltages of the interleaved converter, the voltage of the capacitor has to be controlled. In this paper, a simple boost converter is used for this purpose. The boost converter transfers the leakage energy stored in this clamp capacitor (Cc) to the output and maintains its voltage to a desired clamp voltage level. So, the power rating of the clamp boost converter is decided by the maximum total leakage energy of the interleaved converters. It can be noted that unlike the regular boost converters, which have a fixed input voltage and a variable output voltage, this clamp boost converter has a fixed output voltage but a variable input voltage. This is because the total leakage energy of the interleaved converters is very small compared to the total output power of the interleaved converters. Therefore, the voltage at the output of the clamp boost converter is decided by the interleaved coupled-inductor boost converters.

The inductor and capacitor is given by,

$$L = K (1-K) R / f = V_s K / f I$$

$$C = K / f R = K I / V f$$

The duty ratio of the clamp boost converter can be controlled to discharge the leakage energy stored in the clamp capacitor (Cc) to the output dc bus and maintain its input voltage to a reference clamp voltage level. The clamp voltage level decides the voltage stresses on the switches of the coupled-inductor boost converters. With low switch voltage stress, the converter can be designed to deliver power at high efficiency even when considerable amount of leakage inductance is present in the couple inductors. The clamp boost converter can be operated either in continuous conduction mode (CCM) or in discontinuous conduction mode (DCM). Under CCM, the switching losses are more than the switching losses under DCM. However, the conduction losses under the DCM are more than the conduction losses under the CCM. The clamp boost converter, considered in this study, processes small amount of power obtained from the leakage inductances of the interleaved converters and the voltage level at the clamp capacitor (Vcmin) is quite higher than input voltage level (Vi). Therefore, the average inductor current of the clamp boost converter is small. But the MOSFET of the clamp boost converter switches at high voltage levels. Therefore, in this paper, the clamp boost converter is chosen to operate in DCM to reduce the losses in the clamp boost converter.

### IV. Modes of operation

Consider the non-ideal coupled-inductor boost converters are operated under continuous conduction mode and a boost converter is used for active clamping of the interleaved converters. Under this condition, there are mainly three modes of operation in one switching cycle of a coupled-inductor

boost converter. The operation modes for one of the interleaved cell are shown in Fig. 4, 5, 6. The non-ideal coupled inductors of the interleaved phases can be modeled by a magnetizing inductor ( $L_{m1}$ ), which is connected in parallel with an ideal transformer and a series leakage inductor ( $L_{l1}$ ). The turns ratio of the transformer is equal to the primary to the secondary turns ratio ( $1:N$ ) of the coupled inductor. The value of the magnetizing inductance can be obtained by subtracting the leakage inductance value from the primary winding inductance value of the coupled inductor. The input current and the output current of the interleaved phase are defined in this equivalent model. These operation modes are discussed as follow.

### Stages of Operation

#### Stage 1 ( $t \in [t_0, t_1]$ )

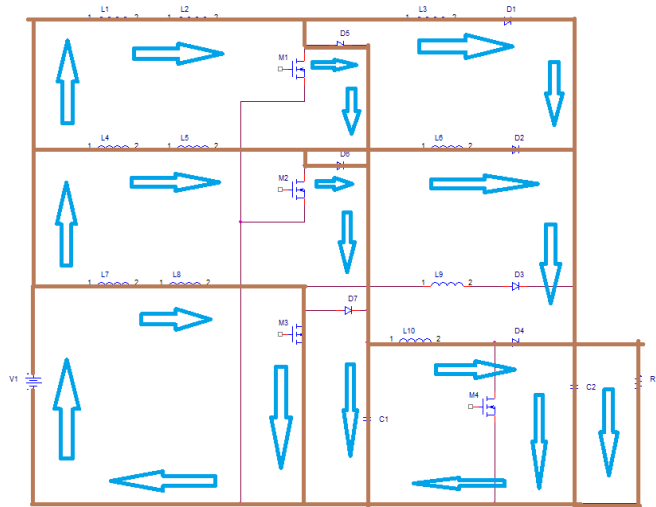


Fig. 4 Stage 1 Operation

This stage begins when the switch S1 is turned on. The output diode D1 is reverse biased, and the input voltage  $V_i$  charges the primary inductor ( $L_{m1}$ ) and the leakage inductor ( $L_{l1}$ ). The input current and the output current of the interleaved phase are defined in this equivalent model. The leakage energies are discharged by the clamping diodes and collected in the capacitor  $C_c$ . The clamping voltage will appear across the output voltage

#### Stage 2 ( $t \in [t_1, t_2]$ )

This stage starts when the switch S1 is turned off. The leakage inductor ( $L_{l1}$ ) forward biases the clamp diode  $D_{c1}$  and the energy stored in the leakage inductor is discharged to the clamp capacitor  $C_c$ . This causes a discharge current spike. The peak of this current is equal to the maximum value of the input current reached at the end of stage-1. At the same instant, when the switch S1 is turned off, the stored energy in the magnetizing inductor ( $L_{m1}$ ) forward biases diode D1 at the secondary side of the coupled inductor.

The voltage difference between the converter output and the input ( $V_o - V_i$ ) is divided as per the turns ratio of the ideal transformer and the voltage at the point A. It can be noted that the fall rate of the leakage current is decided by the voltage difference between the clamp capacitor voltage and the

voltage at the node A. The slope of the input and the output current of the converter during stage-2 are defined by the slopes of the magnetizing current and the leakage inductor current.

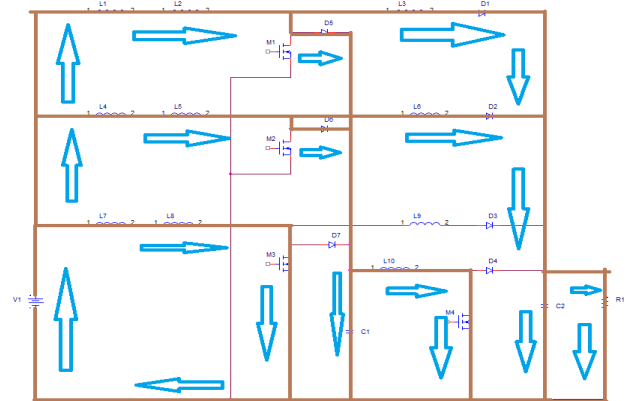


Fig. 5 Stage 2 Operation

#### Stage 3 ( $t \in [t_2, t_3]$ )

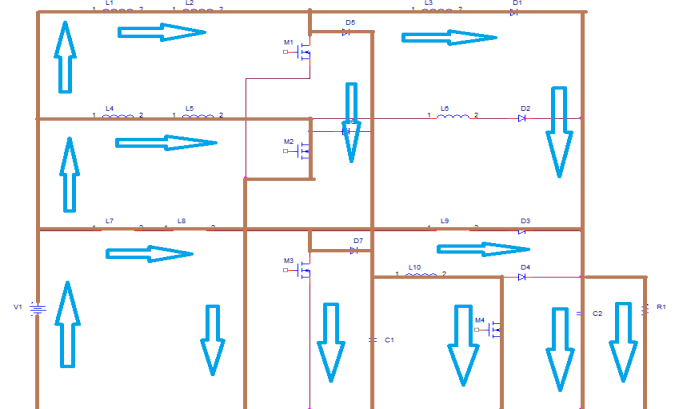


Fig. 6 Stage 3 Operation

This stage begins when the leakage inductor current value has become zero, and the leakage energy is completely discharged. The clamp diode  $D_{c1}$  is reverse biased by the clamp voltage  $V_c$ . The output diode D1 remains forward biased and the voltage at the point A. The energy to the output is transferred from the magnetizing inductor and from the source. The switch S1 remains turned off. The leakage energies are discharged by the clamping diodes and collected in the capacitor  $C_c$ . The clamping voltage will appear across the output voltage.

### V. Simulation Results

The converter consists of three interleaved coupled-inductor boost converters and a common clamp boost converter. In each interleaved cell, three MOSFETs are connected in parallel to realize the switch. It can be seen that the high voltage spikes caused by the leakage inductors can be successfully reduced to a lower level by the proposed clamp boost converter. The measured output voltage is shown in Fig. 8. The simulation results show that the proposed converter can successfully handle the high-input current and perform voltage-step-up operation at a high efficiency. It has been found that with the switches of lower voltage rating, the

recovered leakage energy, and the other benefits of an ideal coupled-inductor boost converter and interleaving, the converter can achieve high efficiency for high-step-up power conversion.

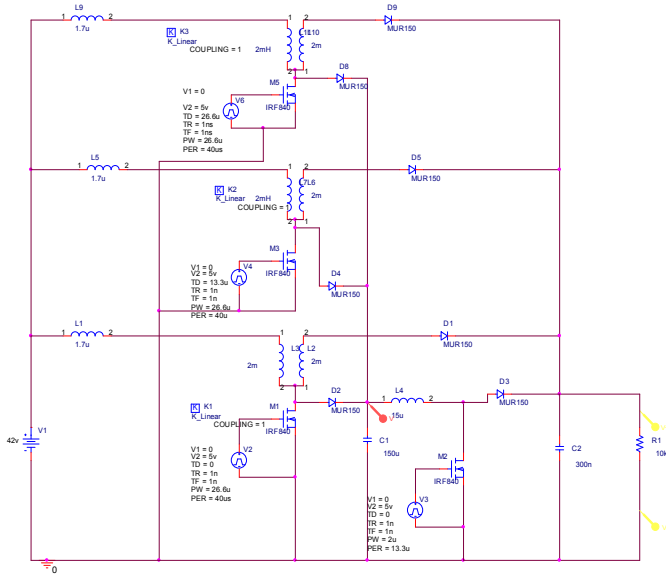


Fig. 7. Interleaved Coupled Inductor Boost Converter

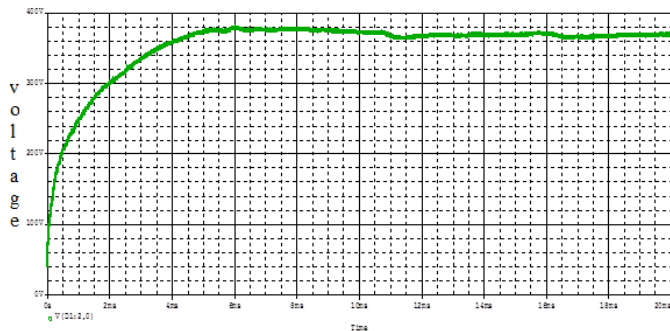


Fig. 8. Output Voltage

**VI. EXPERIMENTAL RESULTS**

In high current or high power application, interleaving of boost converters are well established. To take benefit of the advantages of interleaving, interleaved coupled-inductor boost converter with a common active clamp circuit can be used. In this clamp circuit, the energy stored in the leakage inductance is discharged directly to the output by the parallel diode, and the switch voltage is clamped to the output voltage. The block diagram of hardware is shown in Fig. 9. A prototype of interleaved coupled-inductor boost converter with a common clamp boost converter is developed and tested. The prototype is shown in Fig. 11.

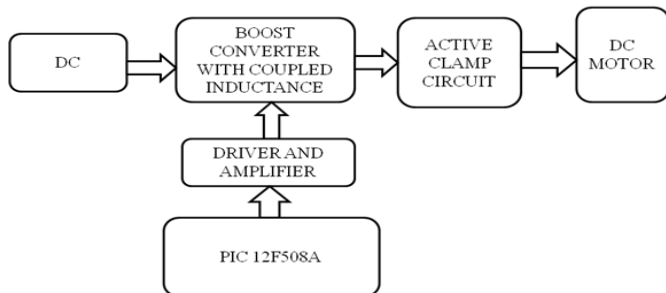


Fig. 9. Block Diagram

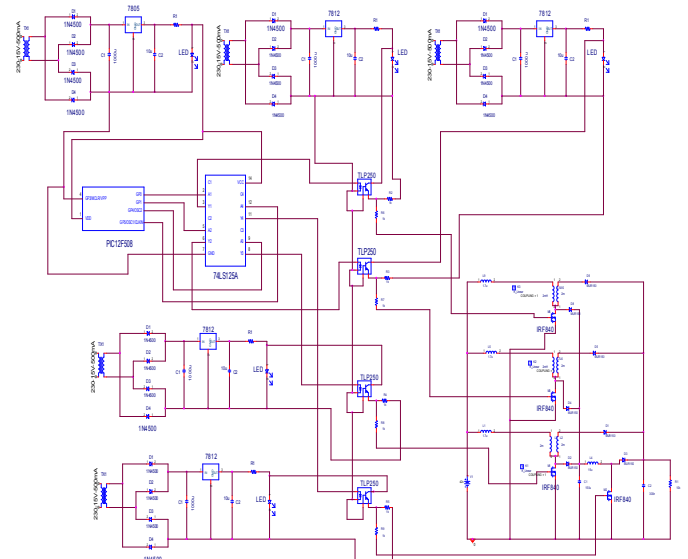


Fig. 10. Proposed Interleaved Boost Converter

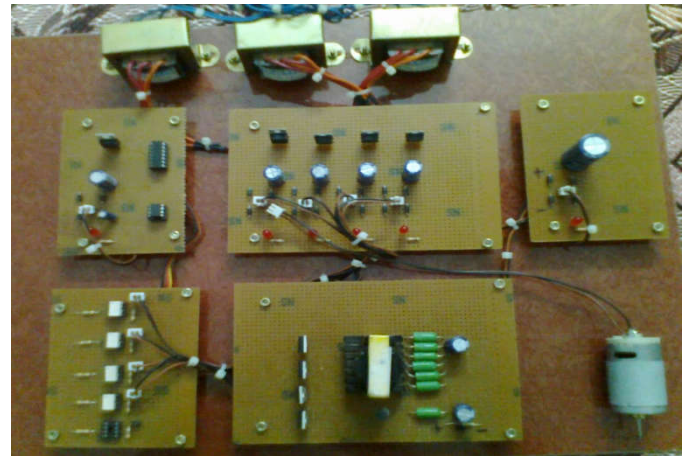


Fig. 11. Prototype of Interleaved Coupled Inductor Boost Converter

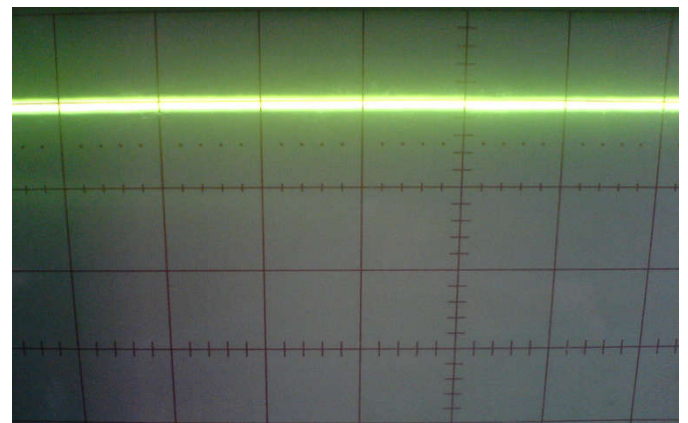


Fig. 12 Voltage Waveform

**VII. Conclusion**

Coupled-inductor boost converters can be interleaved to achieve high-step-up power conversion without extreme duty ratio operation while efficiently handling the high-input current. In a practical coupled-inductor boost converter, the switch is subjected to high voltage stress due to the leakage

inductance present in the non-ideal coupled inductor. The presented active-clamp circuit, based on single boost converter, can successfully reduce the voltage stress of the switches close to the low-level voltage stress offered by an ideal coupled-inductor boost converter. The common clamp capacitor of this active-clamp circuit collects the leakage energies from all the coupled-inductor boost converters, and the boost converter recycles the leakage energies to the output. Detailed analysis of the operation and the performance of the proposed converter were presented in this paper. It has been found that with the switches of lower voltage rating, the recovered leakage energy, and the other benefits of an ideal coupled-inductor boost converter and interleaving, the converter can achieve high efficiency for high-step-up power conversion. A prototype of interleaved coupled-inductor boost converter with a common active clamp circuit was implemented and the results are obtained.

## REFERENCES

- [1] Q. Zhao and F. C. Lee, "High-efficiency, high step-up DC-DC converters," *IEEE Trans. Power Electron.*, vol. 18, no. 1, pp. 65–73, Jan.2003.
- [2] S. Dwari and L. Parsa, "A novel high efficiency high power interleaved coupled-inductor boost DC-DC converter for hybrid and fuel cell electric vehicle," in *Proc. IEEE Veh. Power Propulsion Conf. 2007*, pp. 399–404.
- [3] W. Li and X. He, "An interleaved winding-coupled boost converter with passive lossless clamp circuits," *IEEE Trans. Power Electron.*, vol. 22, no. 4, pp. 1499–1507, Jul. 2007.
- [4] G. C.-Lopez, A. J. Forsyth, and D. R. Nuttall, "Design and performance evaluation of a 10-kW interleaved boost converter for a fuel cell electric vehicle," in *Proc. IEEE Power Electron. Motion Control Conf.*, Aug. 2006, vol. 2, pp. 1–5.
- [5] J. Marshall and M. Kazerani, "Design of an efficient fuel cell vehicle drive train, featuring a novel boost converter," in *Proc. IEEE Ind. Electron. Soc Annu. Conf.*, Nov. 2004, pp. 1229–1234.
- [6] W. Rong-Jong and D. Rou-Yong, "High step-up converter with coupled-inductor," *IEEE Trans. Power Electron.*, vol. 20, no. 5, pp. 1025–1035, Sep. 2005.
- [7] J. Bauman and M. Kazerani, "A comparative study of fuel cell-battery, fuel cell-ultracapacitor, and fuel cell-battery-ultracapacitor vehicles," *IEEE Trans. Veh. Technol.*, vol. 57, no. 2, pp. 760–769, Mar. 2008.
- [8] I. Barbi and R. Gules, "Isolated DC-DC converters with high- output voltage for TWTA telecommunication satellite applications," *IEEE Trans. Power Electron.*, vol. 18, no. 4, pp. 975–984, 2003.
- [9] E. J. Cegnar, H. L. Hess, and B. K. Johnson, "A purely ultracapacitor energy storage system hybrid electric vehicles utilizing a based DC-DC boost converter," in *Proc. Appl. Power Electron. Conf. Expo.*, IEEE, 2004, vol. 2, pp. 1160–1164.
- [10] N. Mohan, T. M. Undeland, and W. P. Robbins, *Power Electronics*, 3rd ed. New York: Wiley, 2002.
- [11] C. Chang and M. A. Knights, "Interleaving technique in distributed power conversion systems," *IEEE Trans. Circuits Syst. I: Fund. Theory Appl.*, vol. 42, no. 5, pp. 245–250, May 1995.
- [12] M. T. Zhang, M. M. Jovanović, and F. C. Lee, "Analysis and evaluation of interleaving techniques in forward converters," *IEEE Trans. Power Electron.*, vol. 13, no. 4, pp. 690–698, Jul. 1998.
- [13] Jungwan Choi, Hanju Cha and Byung-Moon Han, "A three phase interleaved DC-DC converter with active clamp for fuel cells," *IEEE Trans. Power Electron.*, vol. 25, no. 8, pp. 2115–2123, Aug. 2010.
- [14] S. K. Changchien, T. J. Liang, J. F. Chen and L. S. Yang, "Novel high-step-up DC-DC converter for fuel cell energy conversion system," *IEEE Trans. Ind. Electron.*, vol. 57, no. 6, pp. 2007–2017, Jun. 2010.
- [15] Wuhua Li, Yi Zhao, Yan Deng, X. He, "Interleaved converter with voltage multiplier cell for high step-up and high-efficiency conversion," *IEEE Trans. Power Electron.*, vol. 25, no. 9, pp. 2397–2408, Sep. 2010.
- [16] Shin H. B, "Small-signal analysis of multiphase interleaved boost converter with coupled inductors," *IEEE Trans. Power Electron.*, vol. 152, no. 5, pp. 1161–1170, Sep. 2005.
- [17] Po-Wa Lee, Yim-Shu Lee, Cheng D. K. W, Xiu-Cheng Liu, "Steady-state analysis of an interleaved boost converter with coupled inductors," *IEEE Trans. Ind. Electron.*, vol. 47, no. 4, pp. 787–795, Aug. 2000.
- [18] Y. Zhao, W. Li, Y. Deng, X. He, "High step-up boost converter with passive lossless clamp circuit for non-isolated high step-up applications," *IEEE Trans. Power Electron.*, vol. 4, no. 8, pp. 851–859, Sep. 2011.

\*\*\*\*\*